

# Chapter 4

## Methodology: Data Acquisition, Reduction and Measurement

This chapter presents the method of data collection and data reduction process. The reduction processes that we carried out are normalisation, heliocentric correction and telluric lines removal of H $\alpha$ . All methods in the reduction process as well as the measurements of the lines' profile that were explained in this chapter are mainly using Image Reduction and Analysis Facilities (IRAF) routine task jobs. The methodology of the evolutionary study of this star was also explained in the last part of this chapter.

### 4.1 THE SPECTRA OF $\delta$ -SCORPII

Data of the program star in this study were taken from the archive Be Star Spectra (BeSS) Database. This database is maintained at the LESIA laboratory of the Observatoire de Paris-Meudon. All spectra available in the database have already been calibrated and are ready for further analysis. In this study, we have made use of the data of  $\delta$ -Scorpii in the optical range from 2007 to 2011. All data used in this study are listed in Appendix A.

Table 4.1 shows the summary of Echelle data for  $\delta$ -Scorpii with the list of lines of interest; however, not all the lines of interest were used in this study. Column 1 in Table 4.1 lists the filenames of the data that have been written in the format of *\_deltasco\_20yymmdd\_xxx\_zz.fits*. The 20yymmdd represents the year, month and day,

followed by the order number in the Echelle spectrograph that is denoted by xxx\_zz. Columns 2 and 3 show the start and end wavelengths, respectively. Column 4 shows the lines of interest that are among the prominent lines in the wavelength range and column 5 notes the physical characteristic of the line profile: em(dp) for emission line with double-peaked and ab for absorption line.

**Table 4.1** – Summary of data taken using Echelle spectrograph. First column is the image name with observation date, 20yymmdd and number of order, xxx\_zz, column 2 and 3 are the start and end wavelength of each order, column 3 lists all the line of interest and column 4 notes the profile features: em(dp) – emission line (double peak); ab – absorption line.

Image name	w1 (Å)	w2(Å)	Lines of interest	Remarks
_deltasco_20yymmdd_xxx_32.fits	6893.307	7119.284	HeI(7065)	em(dp)
_deltasco_20yymmdd_xxx_34.fits	6484.348	6714.325	Haplha(6562), HeI(6678)	em(dp)
_deltasco_20yymmdd_xxx_35.fits	6320.365	6509.346	SiII(6347,6371)	em(dp)
	5819.415	5999.397	HeI(5876), NaI(5889,5895)	HeI-em(dp), NaI-ab
_deltasco_20yymmdd_xxx_45.fits	4943.503	5057.492	HeI(5016), FeII(5018)	em(dp)
_deltasco_20yymmdd_xxx_46.fits	4828.515	4955.502	H-beta(4860), HeI(4921)	Hbeta- em(dp), HeI- ab
_deltasco_20yymmdd_xxx_48.fits	4629.535	4744.523	OII(4649),HeII(4686)	ab
_deltasco_20yymmdd_xxx_50.fits	4445.553	4550.543	HeI(4471), MgII(4481)	ab
_deltasco_20yymmdd_xxx_51.fits	4364.561	4453.552	HeI(4387), OII(4414)	ab
_deltasco_20yymmdd_xxx_52.fits	4274.670	4374.560	H-gamma(4340)	em(dp)

## 4.2 DATA REDUCTION

The preparations of the lines' profile measurements for the analysis were done using Image Reduction and Analysis Facilities (IRAF). Those preparations are spectral normalisation, removing the telluric lines and heliocentric correction. The procedure for heliocentric correction is explained in the subtopic of radial velocity measurement.

### 4.2.1 Spectral normalisation

The intensity of a 1-D profile is generally high as the scale represents the sum of the pixel values calculated after the binning operation. In order to handle reasonable

values, it is strongly recommended to normalise the intensity profile. In IRAF, the normalisation process can be done using interactive curve fitting tools (ICFIT). The normalisation process makes the continuum level become unity. This is performed by fitting a smooth function through the continuum and dividing the spectrum by this fit. In this work, we used spline3 function as a curve to fit the continuum. During the process we can change its function order to find a moderate RMS value. Figure 4.1 shows the normalisation process of the spectral profiles.

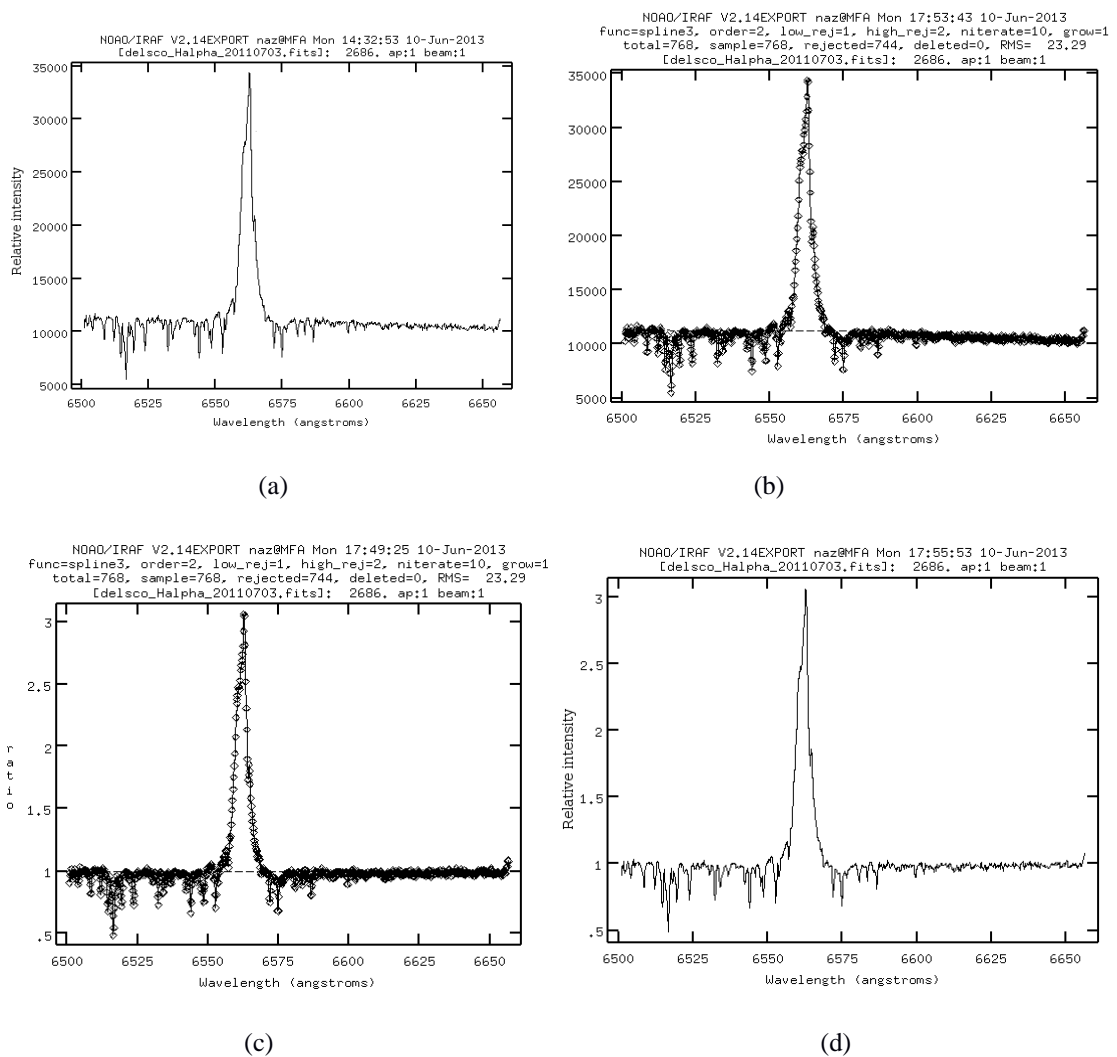


**Figure 4.1** – Normalisation process. (a) Original profile (b) Spline3 function with order 2 is applied to the continuum profile. (c) Curve fitting ratio profile shows the ratio of the spectral profile over the function. (d) A normalised profile.

#### 4.2.2 Telluric lines removal

In the visible region, the water vapour lines of the Earth's atmosphere mostly appear on the left of the  $H_{\alpha}$  line and slightly on the other side of the line. These telluric lines, if severely affected, might obstruct the analysis on the line profile. Thus, the removing of telluric lines is highly recommended. In removing the telluric lines, we employed the synthetic telluric line spectrum, which is taken from the Ritter Observatory archive database, as shown in Figure 4.2.

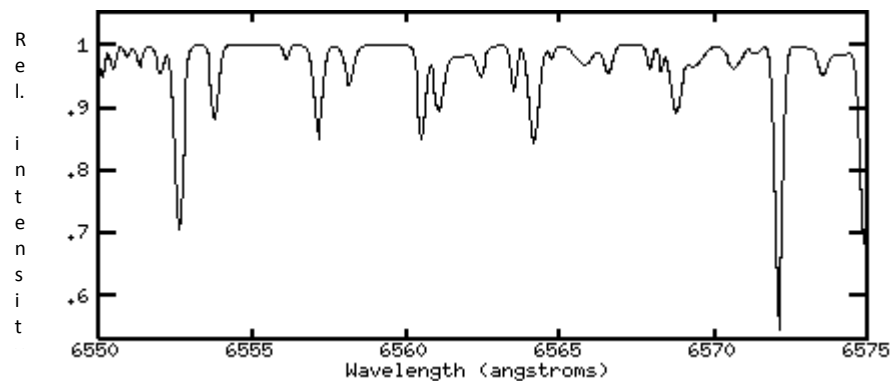


**Figure 4.2** – Synthetic telluric line spectrum in the range of  $H_{\alpha}$  line.

The telluric lines correction in this study was only carried out in the  $H_{\alpha}$  region, as this region might be highly affected by the Earth's atmospheric lines compared with other regions. Figure 4.3 shows the process of telluric line correction of the  $H_{\alpha}$  line profile – (a) the contaminated raw profile of  $H_{\alpha}$  with telluric lines, (b) the removal process of telluric lines. The above panel in (b) shows the resulted profile in 3 different scales: the profile at the centre is corrected using the current scale factor which is automatically obtained by the IRAF telluric removal task job, the upper and lower profiles represent the upper and lower limits of the scale factors i.e  $\pm 0.1$ . The lower panel in (b) and (c) respectively shows the telluric line spectra used in the correction process and the raw  $H_{\alpha}$  profile, and (d) shows the corrected  $H_{\alpha}$  profile.

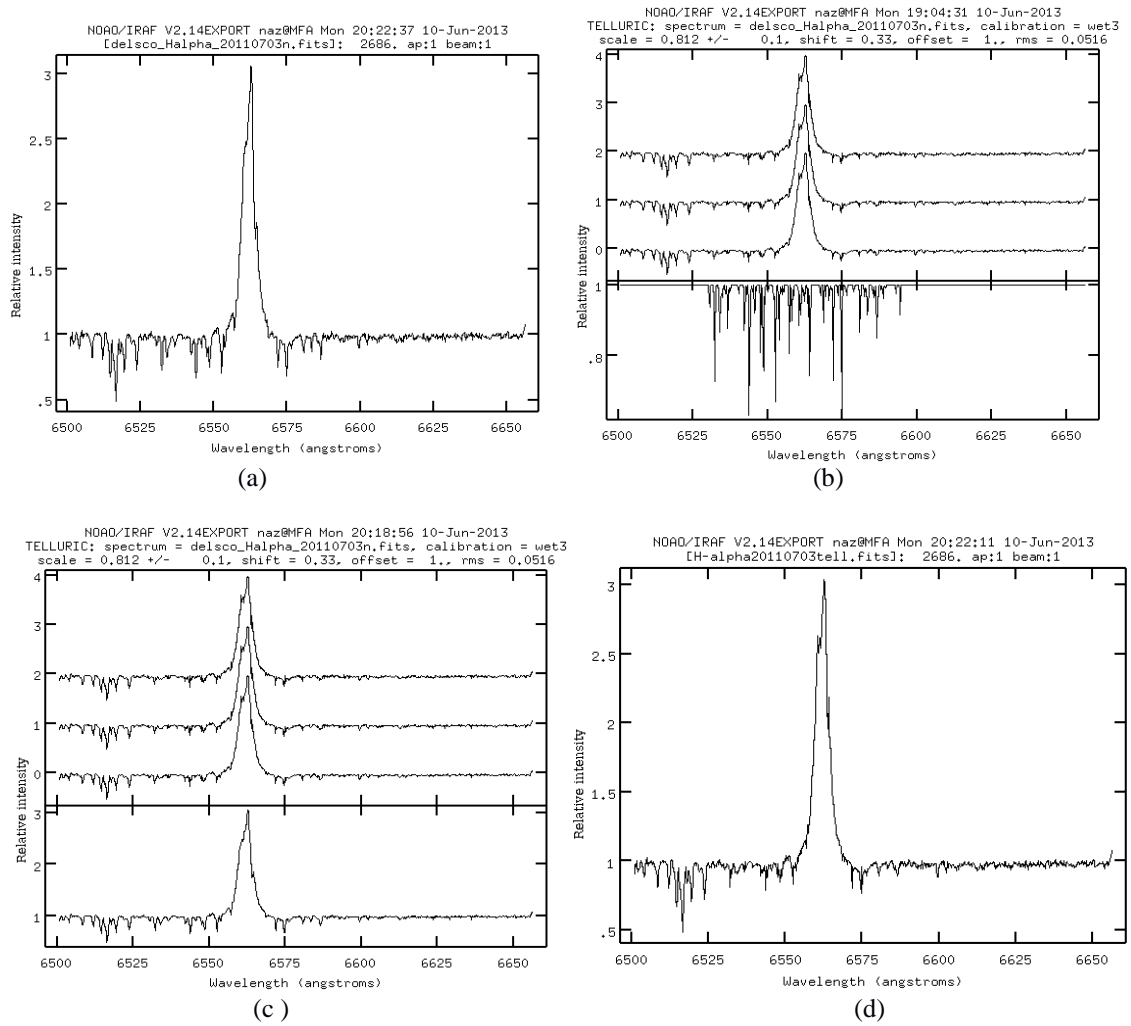


**Figure 4.3** – Telluric lines correction. (a) A raw H $\alpha$  profile. (b) and (c) Telluric lines removal is carried out interactively using IRAF task routine. The telluric line spectrum and raw profile can be toggled out in the lower panel. (d) Profile of H $\alpha$  after the correction.

## 4.3 PROFILE MEASUREMENTS

### 4.3.1 Profile fitting

The spectrum profile of a stellar atmosphere can usually be fitted with certain probability distributions, such as Gaussian, Lorentzian or Voigt. The fitting process enables us to determine the *FWHM*, *EW*, centre of profile, continuum and intensity of the line centre. In an IRAF, we can choose the functions to find the best fit to the spectral profile. For this work, the Voigt function was found more useful in fitting the observed line profile compared with the other functions.

The reason for this is that by the nature of the Gaussian and Lorentzian functions, the shape of the centre of the profile is close to Gaussian whereas the wings are dominated by the Lorentzian. These characteristics are very useful in measuring the spectral profile of Be stars. Most of the profiles of Be stars are very much affected by stellar wind and the movement of gas in their extended atmospheres, which causes the profiles to have such a wing on both sides. The features of the profile are illustrated in Figure 5.4.

#### 4.3.2 Implementation of Voigt function

The Voigt function is the convolution of two probability distributions: a Gaussian  $G(x)$  and a Lorentzian  $L(x)$ . These functions will be normalised to unity:

$$\int_{-\infty}^{\infty} f(x) dx = 1$$

where  $x$  is the independent variable (wavelength, frequency, intensity, etc.) and  $f$  refers to the function of interest. The normalised distributions can then be written as follows:

$$G(x) = \frac{\sqrt{\ln 2}}{\sqrt{\pi} \sigma_G} \exp\left[-\ln 2 \left(x/\sigma_G\right)^2\right] \quad (4.1)$$

and

$$L(x) = (1/\pi \sigma_L) \sigma_L^2 / (x^2 + \sigma_L^2) \quad (4.2)$$

In both functions,  $\sigma$  is represented as full width at half maximum and the subscripted indexes  $G$  and  $L$  refer to the Gaussian and Lorentzian distribution, respectively. In IRAF, the Voigt function can generally be expressed as eq. (4.3):

$$I(\mu) = \int G(\mu')L(\mu - \mu')d\mu \quad (4.3)$$

Eqs. (4.1) and (4.2) were then assigned into eq. (4.3) to form:

$$I(\mu) = \frac{\sqrt{\ln 2}\sigma_L}{\pi^{3/2}\sigma_G} \int_{-\infty}^{\infty} \frac{\exp[-\ln 2(\mu'/\sigma_G)^2]}{(\mu - \mu')^2 + \sigma_L^2} d\mu' \quad (4.4)$$

Let the dimensionless parameters  $p$ ,  $q$  and  $y$  be defined as follows:

$$p = \sqrt{\ln 2}\sigma_L/\sigma_G \quad (4.4)$$

$$q = \sqrt{\ln 2}\mu/\sigma_G \quad (4.5)$$

and

$$\mu = \sqrt{\ln 2}\mu'/\sigma_G \quad (4.6)$$

Eq. (4.4) can be written in the form:

$$I(p, q) = \frac{p^2}{\sigma_L\pi^{3/2}} \int_{-\infty}^{\infty} \frac{\exp[-(y-q)^2]}{(y-q)^2 + p^2} dy \quad (4.7)$$

This form represents the smearing of a Gaussian profile with a Lorentzian profile. Therefore, it has a Gaussian shape near to the line centre, i.e., at  $q=0$  owing to the thermal Doppler shifts and an extended Lorentzian at the wings owing to disturbances

by other particles (damping wing). The process of fitting is done by integrating the functions simultaneously.

#### 4.3.3 Equivalent width ( $EW$ ) and full width at half maximum ( $FWHM$ )

Equivalent width  $EW_\lambda$  was introduced by Minnert et al. (1940) as a line-strength parameter to measure qualitatively the profile growth of an emission or absorption feature, which measures the quantity of light that is cut out from the continuum of a star with an emission line or absorption line by emission or absorption processes. Mathematically, the line strength is the integral of the depth over the wavelength range of the spectral line as eq.(4.8):

$$EW_\lambda \equiv \int_{\lambda_1}^{\lambda_2} \frac{I_c - I(\lambda)}{I_c} d\lambda \quad (4.8)$$

where  $I_c$  is the relative intensity of the continuum,  $I(\lambda)$  is the relative intensity of the line and  $\lambda_1$  and  $\lambda_2$  are the lower and upper wavelength limit of the observed line, respectively. According to relation (4.8), the  $EW$  of an emission line is measured negatively and positively for an absorption line. Geometrically, it is equivalent with the area of the considered line under the normalised continuum.

Full width at half maximum ( $FWHM$ ) is used to describe a measurement of the width of an object or a spectral line when that object or line does not have sharp edges. The width is measured at half level between the continuum and the peak of the line. The  $FWHM$  is expressed in wavelength units or can be converted into speed units by

multiplying the *FWHM* (in wavelength units) with  $c$  and divided by  $\lambda$ , where  $c$  is the speed of light and  $\lambda$  is the line of interest.

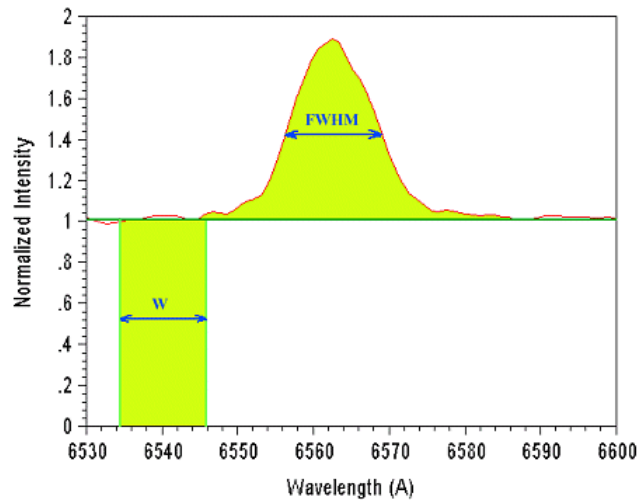


**Figure 4.4** – Definition of equivalent width, labeled as  $W$  and full width at half maximum (*FWHM*).

In the real process, the measurement of *EW* and *FWHM* usually employs the probability distributions, namely Gaussian, Lorentzian or Voigt. In the case of early type Be stars, where the line profile may be affected by a strong stellar wind from the star at the centre, the Voigt function is likely to fit very well on the line profile. Figure 4.2 shows the functions fitted over the sample of the spectral line. The Gaussian and Voigt sometimes have the same profile, as shown in the figure.

Occasionally, the emission lines appear in asymmetrical double-peak or single-peak profile. The measurement of *EW* on the profile becomes complicated when using the distribution functions. Thus, to avoid the complication on the double peak and asymmetric profile, we used a direct integration in measuring the *EW*. This technique is an alternative and is the simplest way in IRAF for obtaining the *EW* of a spectral line.

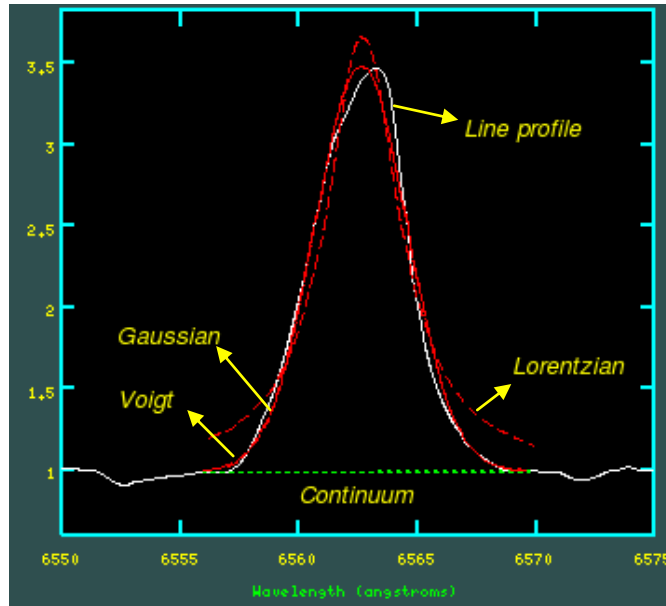


**Figure 4.5** – Distribution function is used to measure the *EW* and *FWHM* of the line profile. Usually, the Lorentzian function itself cannot fit the line profile very well unless it is combined with the Gaussian to become the Voigt function. In the graph, the Gaussian and Voigt functions exhibit better fitting to the line profile than the Lorentzian function does.

Regarding the *FWHM* of the double-peak profile, there are two cases considered for this study: firstly, for a close separation, it is a complicated process to find the *FWHM* for each peak. Hence the *FWHM* is determined by employing either Gaussian or Voigt function whichever fit to most of the line features. In this case we ignored the double-peak feature because the difference in the relative intensity of each peak is small for  $H_{\alpha}$ , thus the location of each *FWHM* in the line profile is very close. Figure 4.3 shows the fitting process in determining the *FWHM*.

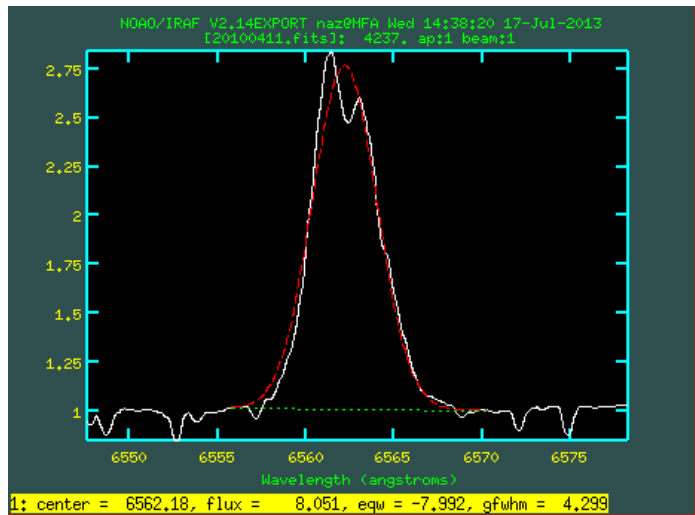


**Figure 4.6** – Measurement of  $FWHM$  on the close separation peak.  $FWHM$  is obtained by fitting either Gaussian or Voigt function to the line profile that represent by the dash red line with respect to its continuum line, the dash green line at the bottom of the line profile.

Secondly, if the double peak is well separated and each peak has its own  $FWHM$ , then the  $FWHM$  is obtained by summing the  $FWHM$  from each peak. This case was not found in the Balmer lines, particularly  $H_{\alpha}$ . For the case of an absorption line, the measurements of  $EW$  and  $FWHM$  have also been done using the same technique.

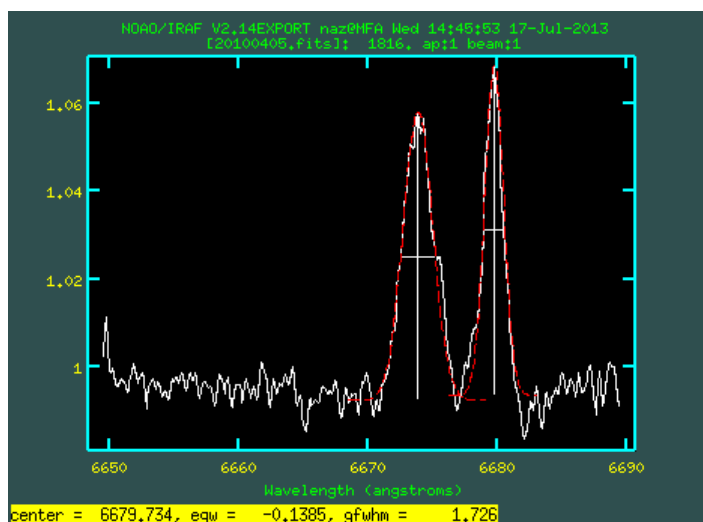


**Figure 4.7** – Measurement of  $FWHM$  on a well separated double peak.  $FWHM$  is obtained by summing the  $FWHM$  of each peak. It was mostly found in HeI  $\lambda 6678$ .

#### 4.3.4 Radial velocity

Radial velocity is determined by applying the Doppler shift equation on the line of interest as follows:

$$v = \frac{(\lambda - \lambda_o)}{\lambda_o} \times c \quad (4.9)$$

where  $v$  is the radial velocity,  $\lambda$  and  $\lambda_o$  are the line of interest and line at rest, respectively and  $c$  is the speed of light. By applying the distribution function on the line profile, the line centre can be obtained but before we can use the line centre for measuring its radial velocity, the heliocentric correction must be performed on the spectra.

#### 4.3.5 Heliocentric correction

In correcting for the effect of the Earth's rotation with respect to the Sun, we need to know the required correction value for the spectra. This value can be found in the image header quoted as BSS\_RQVH in km/s unit for all data taken from the database. The heliocentric correction was done in a direct manner. Before the correction value was applied to the spectra, we converted the image into an ASCII file using the IRAF procedure and we changed the wavelength unit into km/s with respect to the line of interest. Then, the value of BSS\_RQVH from the spectra is deducted from each wavelength.

### 4.4 METHODOLOGY OF THE EVOLUTIONARY STUDY OF $\delta$ -SCORPII

In the study of evolutionary status of  $\delta$ -Scorpii, the evolutionary models at certain mass, rotation and metallicity,  $Z$  were created. However, the chosen values of

mass and rotation were rather made at random. The star is then evolved at the same mass and rotation (if possible) but with different metallicity, i.e.,  $Z = 0.02$  and  $0.01$ . We attempt to point or allocate the current status of  $\delta$ -Scorpii on the HR diagram based on its adopted effective temperature and estimated radius, which is calculated using the bolometric flux method.

The evolutionary models were created using EV stellar evolution code. All the steps carried out in the evolution process were referred to the job tasks given and the configuration files that contain the parameters that we can change for the evolution process are shown in Appendix B. The initial mass of this star was chosen randomly but within a certain range. The initial rotation also was chosen randomly, on the proviso that the code can be run or initialised with respect to the initial mass and metallicity and that the rotation rate did not exceed the critical velocity during the course of the evolution. In this work, we are also considering a high rotational velocity character of Be stars during its lifetime in the main sequence band, in which the rotation rate of the star should be faster than 70% of its critical rate. Several parameters, namely surface temperature, luminosity, mass, age, radius, core temperature, rotation period and radiative pressure were extracted from a long strip of the evolution process output to be used in the analysis. The current physical parameters of the star, such as temperature, mass and radius were used as a guide in suggesting the evolutionary models of  $\delta$ -Scorpii.